Journal of Computational Applied Mechanics 2024, 55(3): 485-499

DOI: 10.22059/JCAMECH.2024.377658.1121

RESEARCH PAPER

Vibration Analysis of Sandwich Plates with Hybrid Composite Cores Combining Porous Polymer and Foam Structures

Hussam Raad [a], Emad Kadum Njim [b,*], Muhsin J. Jweeg [c], Muhannad Al-Waily [a], Lazreg Hadji [d], Royal Madan [e]

[a] *Department of Mechanical Engineering, Faculty of Engineering, University of Kufa, 00964, Iraq*
[b] *Ministry of Industry and Minerals, State Company for Rubber and Tires Industries, Najaf, 00964, Iraq*
[c] *Al-Farahidi University, College of Technical Engineering, Baghdad, 00964, Iraq*
[d] *Department of Mechanical Engineering, University of Tiaret, Tiaret, 00213, Algeria*
[e] *Department of Mechanical Engineering, Graphic Era (Deemed to be University), Dehradun 248002, Uttarakhand, India*

Abstract

Sandwich structures are composites comprising a core layer sandwiched between two face layers; each layer has a distinctive characteristic, and the structure can also include composite layers. This study presents an investigation of the free vibration behavior of a cored hybrid sandwich plate. The research demonstrates an analytical and numerical analysis. Sandwich plate models made of aluminum face sheets with reinforced cores are used in this study. The analytical analysis used in this study of a three-layer sandwich plate is based on Kirchhoff's theorem. An additional mathematical model is constructed by dividing the core layer into two parts to form four layers with a hybrid structure. The governing equations to obtain the mechanical properties and natural frequency of the foam composite, as well as open structural and hybrid cores, were used in this study. The numerical analysis of the various composite structures using the modal analysis was performed through ANSYS version 2021-R1. Analytical outcomes reveal that replacing the foam core with an open-cell structure reduces the natural frequency by 25%. However, the hybrid core structure reduces the natural frequency by 27.6%. Also, the ultimate flexural load in the hybrid structure is increased by 127.7% compared to the open-cell structure core. Finally, numerical results are highly consistent with those obtained analytically.

Keywords: Sandwich plate; Composite core; Porous core; Foam structure; Free vibration

1. Introduction

As humans began constructing heavily loaded structures relying on densely impermeable materials like steel under the same stress and boundary conditions, composites like sandwich structures are lighter and more corrosion-resistant than conventional metallic materials. Sandwich structures play a significant role in producing composite products as they appear in almost all application areas [1]. Historically, sandwich structures were the very first functional composite structures. The constant challenge is making a structure as light as feasible, with rapid manufacturing and reducing costs without affecting strength.

A structure must be stabilized to sustain tensile and compressive stresses in tension, torsion, bending, and their combination [2, 3]. Because of the ability to design structures with specific features, cellular structures were created by man to replace traditional materials such as honeycombs [4] and foam structures [5]. As man was inspired by nature, it was already cellular, as evidenced by the presence of bone, coral, and other similar materials. Foam may be made from almost any material, including polymers, metals, composite structures, etc. The structure and substance of any foam's cell walls influence its qualities. Cellular solids are used for thermal insulation, packing, filtration, structural applications, and buoyancy [6].

There has recently been a significant interest in using cellular solids, which serve many functions. The biggest challenge in making these materials so far has been numerous manufacturers' inability to manage content distribution at the cellular level. Cellular substances have distinct benefits over conventional substances and non-cellular polymers. With the advancement of technology in recent years, studies have been carried out on composite materials that are lighter, stronger, and more rigid. A sandwich panel is a structural composite that combines different elements to maximize the structural usefulness of the complete construction. A sandwich requires three main components: a thin, stiff, and strong core. The faces are adhered to the core to transmit load. Sandwiches operate similarly to I-beams, with the faces replacing the flanges and the core taking the place of the web. The sandwich's core is made of a material distinct from the sandwich's faces and provides continuous support for those faces. The faces will create a stress pair to resist the external bending moment. The core resists shearing and stabilizes the faces versus buckle or wrinkle. Face and core adhesion must be strong enough to withstand tension and compression forces [7]. Scientists have paid significant attention to the elastic properties of closed-cell polymeric foam due to its wide use in engineering applications. Many contributions investigated the static and dynamic analysis of foam core sandwich plates; some adopted aluminum as a foam material [8, 9], while others used polyurethane and other materials [10]. Highlighting the critical parameters and the influence of structural foam dynamic response behavior.

Guo et al. [11], investigated the dynamic behavior of aluminum foam sandwich plates under repeated impact loads. In this study, a sandwich plate of upper and lower face aluminum and closed aluminum foam core by epoxy resin adhesion warmed beneath approximately 60°C. An experimental study inferred that the back face sheet still has residual load-carrying capacity even if the front face sheet became cracked. Caglayan et al. [12] studied the impact response of sandwich panels with polymer foam core using a new mathematical model. They focused on the effects of shear-thickening fluids on polymer foam cell morphology, thermal stability, and mechanical performance. Using amorphous silica nanoparticles SiO_2 as a dry powder and polyol with polymeric. The shear thickening fluids-filled PUR foam core sandwich composites responded with lower damage width than neat PU foams.

Ren et al. [13] investigated the dynamic failure of sandwich plates with polyvinyl chloride foam cores when subjected to foam projectile impact. A sandwich structure has a polyvinyl-chloride core at the same area; mass replacing an Al sheet with a composite enhances the impact strength. By boosting the density of PVC foam cores, sandwich plates' impact resistance can be increased. A sandwich plate with a thicker core layer can more effectively extend the dynamic response time of the structure, increasing the energy of the impact impulse and enhancing the protective property of the plates. Koyama et al. [14] used Polyurethane PUR foam, a foamable, lightweight, and waterproof polymer substance. The researcher looks at the dynamic deformation properties of rigid polyurethane foam. According to JGS 0542-2009, the specimens utilized for dynamic deformation tests were cylinders identical to those used in cyclic triaxial testing to determine how dynamically deformable soils are. Under one-dimensional stress circumstances, stiff foam deformed compressively, but under three-dimensional stress conditions, it deformed both in the compression and extension directions. As a result, the dynamic qualities varied. Finite element analysis of laminated composite plates using a higher order shear deformation theory on stress distribution in a five-layer sandwich plate with assumed a continuous displacement across the layers was performed by Hamed Raissi et al. [15]. They used a square, supported sandwich plate based on layerwise theory.

Recently, many researchers studied static and analysis of functionally graded sandwich plates using multiple techniques [16-18]. When sandwich structures are subjected to external stimuli, such as mechanical or acoustic vibrations, free vibration analysis is critical because it allows us to understand their dynamic behavior. An analysis of the free vibrations of SPs can help determine their natural frequencies, mode shapes, and damping characteristics. It is, therefore, necessary to conduct a free vibration analysis of these materials before designing them.

Njim et al. [19] suggested an analytical solution for vibration analysis of a functionally graded material (FGM) sandwich plate. The differential equation of motion for the vibration analysis of the FGM sandwich combined plate is solved to evaluate the natural frequency of the plate with different design parameters. Increasing the gradient index and core thickness increases the natural frequency of the FGM sandwich plate structure. While increasing the thickness of the upper and lower plate parts reduces the strength-to-weight ratio, it also reduces the natural frequency of the porous sandwich plate structure. Maraş and Yaman [20] conducted free vibration of polymeric foam to be used in composite sandwich beam models, offering insights into syntactic foam behavior under dynamic loading conditions using experimental and numerical methods.

In their study, Nguyen et al. [21] examined reinforced polyurethane foam-based composites and studied their mechanical behavior and dynamic characteristics based on a modified strain gradient theory. According to the results, the size effect significantly improves buckling, bending, and free vibration properties. Jiaming Sun et al. [22] developed constitutive damage models for the simulation-free vibration of composite sandwiches with foam-filled cores under a wide range of temperatures and strain rate programs, enhancing the accuracy of foam behavior predictions in complex loading scenarios. Additionally, each service structure must be prepared with different suppression ranges based on specific circumstances, resulting in structures with different vibration suppression ranges. Hence, Zelin Li et al. [23] performed comprehensive theoretical and experimental techniques to examine the nonlinear vibration behaviors of foam-filled honeycomb sandwich cylindrical shells by employing multiple compressive and dynamic loading, providing insights into foam response under dynamic loading conditions.

A five-layer sandwich nanocomposite beam reinforced with graphene platelets (GPLs) and shape memory alloys (SMAs) has been evaluated theoretically by Arabzadeh-Ziari et al. [24] for predicting deflection, buckling, and vibration under high dynamic loading. Ashkan Farazin et al. [25] conducted an experimental investigation on composite sandwich plates with aluminum foam under impact loading, providing valuable data for understanding foam behavior in impact scenarios. The free vibration of composite structures has been extensively studied using various methods such as differential cubature-Newmark method [26], higher-order theories [27], differential quadrature hierarchical finite element method [28], differential quadrature method [29], elasticity approach [30-35], and zigzag shear deformation theory [36]. Nanocomposites are designed to integrate different materials at the nanoscale to create materials with unique properties and functionalities. The structure of nanocomposites is critical in determining their performance and potential applications across various industries [37-39]. L. Shan et al. [40] investigated the influence of the presence of nanoparticles on the dynamic characteristics of composite structures, considering multiple parameters such as volume fraction and geometrical properties. It is found that the uniform dispersion of nanoscale fillers is crucial for achieving these enhanced properties, as clustering can lead to structural defects and failure. Moreover, the detailed study on an experimental study for the effect of hole notched in fracture mechanism of composite structures subjected to quasi-static loading is conducted by C. Chu et al. [41].

Recent developments in materials engineering have achieved remarkable progress, notably through the introduction of functionally graded materials (FGMs). These groundbreaking materials have gained significant attention due to their unique and adaptable properties, which diverge from conventional material design methods. In contrast to homogeneous materials, FGMs feature a continuous and seamless variation in their thermo-mechanical properties, making them exceptionally versatile and distinct [42-44]. Fundamentally, FGMs are designed to possess tailored properties that smoothly transition from one end to another. FGMs represent a significant breakthrough in engineering and science, offering innovative solutions to multifaceted challenges encountered across various industries, including aerospace and biomedical sectors [45]. Moreover, Al-Furjan et al. [46] examined the wave propagation in FGM composite sandwich beams based on modified couple stress and refined zigzag theories.

From the literature, it is found that there are very few investigations on the free vibration analysis of SPs with hybrid composite core combined with porous polymer and foam layers.

This study aims to design and conduct free vibration characterizations for sandwich plates with foam PLA, TPU, and hybrid core open loop structure core. The study is planned to derive the natural frequency equation analytically and verification results using the finite element method with the help of ANSYS software tools.

2. Nomenclature

SPs	Sandwich plates
FGM	Functionally graded materials
CPT	Classical plate theory
PU	Polyurethane foam
SS	Simply supported
PLA	Polylactic acid
TPU	Thermoplastic polyurethane
GPLs	Graphene platelets
SMAs	Shape memory alloys

3. Analytical model

Hybrid material cores merge two or more materials that cannot be distinguished by layers (similar to a skeletal form). Each material has specific mechanical properties and performance, creating a material with a different performance. Analyzing a hybrid core depending on the foam material performance and the open-cell structure, margining them together with the assumptions structure, as shown in Fig. 1. Hooke's Law and plate theory are used to derive the following field equations for stress **[**47**]**;

$$\begin{Bmatrix} M_x \\ M_y \\ M_{xy} \end{Bmatrix} = \int_{-z/2}^{z/2} \begin{Bmatrix} \sigma_x \\ \sigma_y \\ \tau_{xy} \end{Bmatrix} zdz \tag{1}$$

As**,** $\boldsymbol{\sigma_x}$, $\boldsymbol{\sigma_y}$ and $\boldsymbol{\tau_{xy}}$ are the normal and share stresses on the plate. Also, for the part of (ρh) can be expressed as,

$$\rho h = \int_{-z/2}^{z/2} \rho dz \tag{2}$$

As demonstrated in Fig. 2 of the hybrid core as a layer in the sandwich plate, and Fig. 3 shows the laminated dimensions of the sandwich.

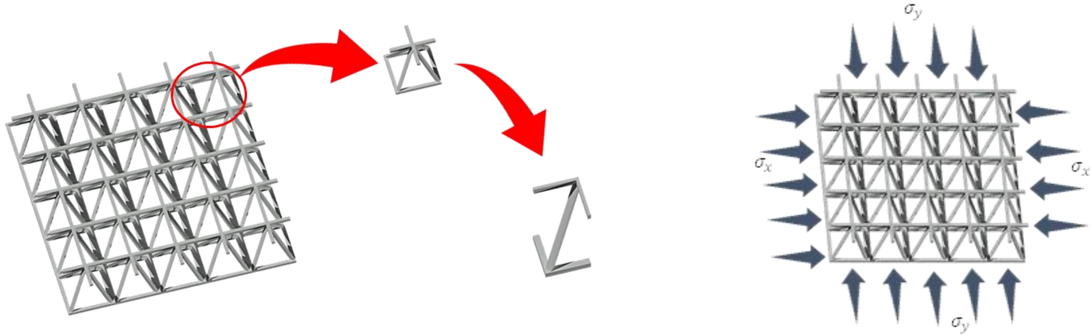

a. Open-cell structure **b. Open cell in the x-y direction**

Fig. 1. The assumed open structure.

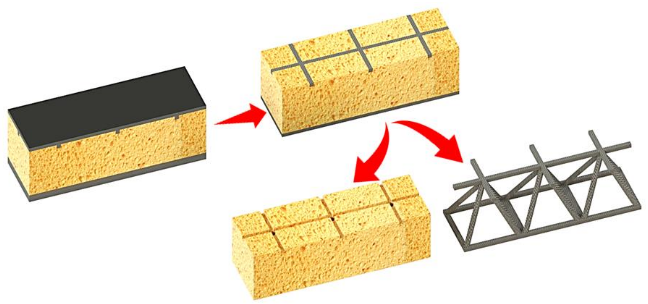

Fig. 2. Hybrid core as a layer in the sandwich plate.

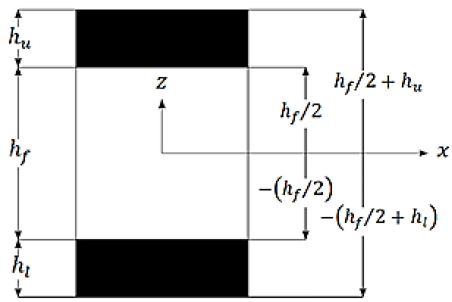

Fig. 3. Geometry of the sandwich layers.

Stress relationships for each layer of the sandwich plate can be expressed in terms of each property, the mechanical properties of upper and lower, as mentioned before, for the foam and cell structure. Mechanical properties of foam core part,

$$E_{xx} = E_{f1} E_{yy} = E_{f2} \tag{3}$$

And,

$$G_{xy} = G_f, \;\; \nu_{xy} = \nu_{f12}, \;\; \nu_{xy} = \nu_{f21} \tag{4}$$

And mechanical properties of the cell core part,

$$E_{xx} = E_{c1} \text{ , } E_{yy} = E_{c2} \tag{5a}$$

And,

$$G_{xy} = G_c$$

Also,

$$\nu_{xy} = \nu_{c12} \text{ , } \nu_{yx} = \nu_{c21} \tag{5b}$$

Then,

$$\begin{Bmatrix} \sigma_{xy} \\ \sigma_{yy} \\ \sigma_{xy} \end{Bmatrix} = -z \begin{Bmatrix} \frac{E_{c1}}{1-\nu_{c12}\nu_{c21}} \frac{\partial^2 w}{\partial x^2} + \frac{E_{c2}\nu_{c12}}{1-\nu_{c12}\nu_{c21}} \frac{\partial^2 w}{\partial y^2} \\ \frac{E_{c1}\nu_{c12}}{1-\nu_{c12}\nu_{c21}} \frac{\partial^2 w}{\partial x^2} + \frac{E_{c2}}{1-\nu_{c12}\nu_{c21}} \frac{\partial^2 w}{\partial y^2} \\ 2G_c \frac{\partial^2 w}{\partial_x \partial_y} \end{Bmatrix} \tag{6}$$

The hybrid core of the foam and the open-cell structure occupy the same space over the same height (h_f); therefore, the integration would be over the height. The integrating equations to obtain the moments and shear components would be,

$$\begin{Bmatrix} M_x \\ M_y \\ M_{xy} \end{Bmatrix} = \begin{Bmatrix} \int_{-\left(\frac{1}{2}h_f + h_1\right)}^{-\left(\frac{1}{2}h_f\right)} (\sigma_x)_1 zdz + \int_{-\left(\frac{1}{2}h_f\right)}^{\left(\frac{1}{2}h_f\right)} (\sigma_x)_f zdz + \int_{-\left(\frac{1}{2}h_f\right)}^{\left(\frac{1}{2}h_f\right)} (\sigma_x)_c zdz + \int_{\left(\frac{1}{2}h_f\right)}^{\left(\frac{1}{2}h_f + h_u\right)} (\sigma_x)_u zdz \\ \int_{-\left(\frac{1}{2}h_f + h_1\right)}^{-\left(\frac{1}{2}h_f\right)} (\sigma_y)_1 zdz + \int_{-\left(\frac{1}{2}h_f\right)}^{\left(\frac{1}{2}h_f\right)} (\sigma_y)_f zdz + \int_{-\left(\frac{1}{2}h_f\right)}^{\left(\frac{1}{2}h_f + h_u\right)} (\sigma_y)_c zdz + + \int_{\left(\frac{1}{2}h_f\right)}^{\left(\frac{1}{2}h_f + h_u\right)} (\sigma_y)_u zdz \\ \int_{-\left(\frac{1}{2}h_f + h_1\right)}^{-\left(\frac{1}{2}h_f\right)} (\tau_{xy})_1 zdz + \int_{-\left(\frac{1}{2}h_f\right)}^{\left(\frac{1}{2}h_f\right)} (\tau_{xy})_f zdz + \int_{-\left(\frac{1}{2}h_f\right)}^{\left(\frac{1}{2}h_f + h_u\right)} (\tau_{xy})_c zdz + + \int_{\left(\frac{1}{2}h_f\right)}^{\left(\frac{1}{2}h_f + h_u\right)} (\tau_{xy})_u zdz \end{Bmatrix} \tag{7}$$

The same idea is applied to density per unit length,

$$\rho h = \int_{-\left(\frac{1}{2}h_f+h_1\right)}^{-\left(\frac{1}{2}h_f\right)} \rho_1 dz + \int_{-\left(\frac{1}{2}h_f\right)}^{\left(\frac{1}{2}h_f\right)} \rho_f\, dz + \int_{-\left(\frac{1}{2}h_f\right)}^{\left(\frac{1}{2}h_f\right)} \rho_c dz + \int_{\left(\frac{1}{2}h_f\right)}^{\left(\frac{1}{2}h_f+h_u\right)} \rho_u dz \tag{8}$$

By multiple integrating the above equations, we obtain,

$$M_x = \left(\begin{array}{l} \displaystyle\int_{-\left(\frac{1}{2}h_f+h_1\right)}^{-\left(\frac{1}{2}h_f\right)} \left(\frac{zE_1}{1-\nu_1{}^2}\left(\frac{\partial^2 w}{\partial x^2}+\nu_1\frac{\partial^2 w}{\partial y^2}\right)\right) zdz + \int_{-\left(\frac{1}{2}h_f\right)}^{\left(\frac{1}{2}h_f\right)} \left(\frac{zE_{f1}}{1-\nu_{f12}\nu_{f21}}\frac{\partial^2 w}{\partial x^2}+\frac{zE_{f2}\nu_{f12}}{1-\nu_{f12}\nu_{f21}}\frac{\partial^2 w}{\partial y^2}\right) zdz + \\ \displaystyle\int_{-\left(\frac{1}{2}h_f\right)}^{\left(\frac{1}{2}h_f\right)} \left(\frac{zE_{c1}}{1-\nu_{c12}\nu_{c21}}\frac{\partial^2 w}{\partial x^2}+\frac{zE_{c2}\nu_{c12}}{1-\nu_{c12}\nu_{c21}}\frac{\partial^2 w}{\partial y^2}\right) zdz + \int_{\left(\frac{1}{2}h_f\right)}^{\left(\frac{1}{2}h_f+h_u\right)} \left(\frac{zE_u}{1-\nu_u{}^2}\left(\frac{\partial^2 w}{\partial x^2}+\nu_u\frac{\partial^2 w}{\partial y^2}\right)\right) zdz \end{array} \right) \tag{9a}$$

$$M_y = \left(\begin{array}{l} \displaystyle\int_{-\left(\frac{1}{2}h_f+h_1\right)}^{-\left(\frac{1}{2}h_f\right)} \left(\frac{E_1}{1-\nu_1{}^2}\left(\nu_1\frac{\partial^2 w}{\partial x^2}+\frac{\partial^2 w}{\partial y^2}\right)\right) zdz + \int_{-\left(\frac{1}{2}h_f\right)}^{\left(\frac{1}{2}h_f\right)} \left(\frac{zE_{f1}\nu_{f12}}{1-\nu_{f12}\nu_{f21}}\frac{\partial^2 w}{\partial x^2}+\frac{zE_{f2}}{1-\nu_{f12}\nu_{f21}}\frac{\partial^2 w}{\partial y^2}\right) zdz + \\ \displaystyle\int_{\left(\frac{1}{2}h_f\right)}^{\left(\frac{1}{2}h_f\right)} \left(\frac{zE_{c1}\nu_{c12}}{1-\nu_{c12}\nu_{c21}}\frac{\partial^2 w}{\partial x^2}+\frac{zE_{c2}\nu_{c12}}{1-\nu_{c12}\nu_{c21}}\frac{\partial^2 w}{\partial y^2}\right) zdz + \int_{\left(\frac{1}{2}h_f\right)}^{\left(\frac{1}{2}h_f+h_u\right)} \left(\frac{zE_u}{1-\nu_u{}^2}\left(\nu_u\frac{\partial^2 w}{\partial x^2}+\frac{\partial^2 w}{\partial y^2}\right)\right) zdz \end{array} \right) \tag{9b}$$

$$M_{xy} = -\left(\begin{array}{l} \displaystyle\int_{-\left(\frac{1}{2}h_f+h_1\right)}^{-\left(\frac{1}{2}h_f\right)} \left(\frac{zE_1}{(1+\nu_1)}\frac{\partial^2 w}{\partial x\partial y}\right) zdz + \int_{-\left(\frac{1}{2}h_f\right)}^{\left(\frac{1}{2}h_f\right)} \left(2zG_f\frac{\partial^2 w}{\partial x\partial y}\right) zdz \\ \displaystyle + \int_{\left(-\frac{1}{2}h_f\right)}^{\left(\frac{1}{2}h_f\right)} \left(2zG_c\frac{\partial^2 w}{\partial x\partial y}\right) zdz + \int_{\left(\frac{1}{2}h_f\right)}^{\left(\frac{1}{2}h_f+h_u\right)} \left(\frac{zE_u}{(1+\nu_u)}\frac{\partial^2 w}{\partial x\partial y}\right) zdz \end{array} \right) \tag{9c}$$

The above component is to be a back substitution in the equation,

$$\frac{\partial^2 M_{xx}}{\partial x^2} + 2\frac{\partial^2 M_{xy}}{\partial x\partial y} + \frac{\partial^2 M_{yy}}{\partial y^2} + \rho h\frac{\partial^2 \omega}{\partial t^2} = 0 \tag{10}$$

Then, it can be expressed as shown,

$$M_x = -\left(\begin{array}{l} \left(\frac{E_1}{1-\nu_1^{\,2}} \left(\frac{h_1^{\,3}}{3} + \frac{h_1^{\,2} h_f}{2} + \frac{h_1 h_f^{\,2}}{4} \right) \left(\frac{\partial^2 w}{\partial x^2} + \nu_1 \frac{\partial^2 w}{\partial y^2} \right) \right) + \left(\left(\frac{h_f^{\,3}}{12} \right) \left(\begin{array}{l} \frac{E_{f1}}{1-\nu_{f12}\nu_{f21}} \frac{\partial^2 w}{\partial x^2} + \\ \frac{E_{f2}\nu_{f12}}{1-\nu_{f12}\nu_{f21}} \frac{\partial^2 w}{\partial y^2} \end{array} \right) \right) \\ + \left(\left(\frac{h_f^{\,3}}{12} \right) \left(\begin{array}{l} \frac{E_{c1}}{1-\nu_{c12}\nu_{c21}} \frac{\partial^2 w}{\partial x^2} + \\ \frac{E_{fc2}\nu_{c12}}{1-\nu_{c12}\nu_{c21}} \frac{\partial^2 w}{\partial y^2} \end{array} \right) \right) + \left(\frac{E_u}{1-\nu_u^{\,2}} \left(\frac{h_u^{\,3}}{3} + \frac{h_u^{\,2} h_f}{2} + \frac{h_u h_f^{\,2}}{4} \right) \left(\frac{\partial^2 w}{\partial x^2} + \nu_u \frac{\partial^2 w}{\partial y^2} \right) \right) \end{array} \right) \tag{11a}$$

$$M_y = -\left(\begin{array}{l} \left(\frac{E_1}{1-\nu_1^{\,2}} \left(\frac{h_1^{\,3}}{3} + \frac{h_1^{\,2} h_f}{2} + \frac{h_1 h_f^{\,2}}{4} \right) \left(\nu_1 \frac{\partial^2 w}{\partial x^2} + \frac{\partial^2 w}{\partial y^2} \right) \right) + \left(\left(\frac{h_f^{\,3}}{12} \right) \left(\begin{array}{l} \frac{E_{f1}\nu_{f12}}{1-\nu_{f12}\nu_{f21}} \frac{\partial^2 w}{\partial x^2} + \\ \frac{E_{f2}}{1-\nu_{f12}\nu_{f21}} \frac{\partial^2 w}{\partial y^2} \end{array} \right) \right) \\ + \left(\left(\frac{h_f^{\,3}}{12} \right) \left(\begin{array}{l} \frac{E_{c1}\nu_{c12}}{1-\nu_{c12}\nu_{c21}} \frac{\partial^2 w}{\partial x^2} + \\ \frac{E_{c2}\nu_{c12}}{1-\nu_{c12}\nu_{c21}} \frac{\partial^2 w}{\partial y^2} \end{array} \right) \right) + \left(\frac{E_u}{1-\nu_u^{\,2}} \left(\frac{h_u^{\,3}}{3} + \frac{h_u^{\,2} h_f}{2} + \frac{h_u h_f^{\,2}}{4} \right) \left(\nu_u \frac{\partial^2 w}{\partial x^2} + \frac{\partial^2 w}{\partial y^2} \right) \right) \end{array} \right) \tag{11b}$$

$$M_{xy} = -\left(\begin{array}{l} \left(\frac{E_1}{(1+\nu_1)} \left(\frac{h_1^{\,3}}{3} + \frac{h_1^{\,2} h_f}{2} + \frac{h_1 h_f^{\,2}}{4} \right) \frac{\partial^2 w}{\partial x \partial y} \right) + G_f \left(\left(\frac{h_f^{\,3}}{6} \right) \frac{\partial^2 w}{\partial x \partial y} \right) + \\ G_c \left(\left(\frac{h_f^{\,3}}{6} \right) \frac{\partial^2 w}{\partial x \partial y} \right) \left(\frac{E_u}{(1+\nu_u)} \left(\frac{h_u^{\,3}}{3} + \frac{h_u^{\,2} h_f}{2} + \frac{h_u h_f^{\,2}}{4} \right) \frac{\partial^2 w}{\partial x \partial y} \right) \end{array} \right) \tag{11c}$$

$$\rho h = \rho_1 h_1 + \rho_f h_f + \rho_c h_f + \rho_u h_u \tag{12}$$

After integration was done, back substitution of the resultant in the equilibrium Eq. (10) leads to,

$$\left(\begin{array}{l}\left(\begin{array}{l}\frac{E_1}{1-\nu_1^2}\left(\frac{h_1^3}{3}+\frac{h_1^2h_f}{2}+\frac{h_1h_f^2}{4}\right)+\frac{E_{f1}}{1-\nu_{f12}\nu_{f21}}\left(\frac{h_f^3}{12}\right)+\\ \frac{E_{c1}}{1-\nu_{c12}\nu_{c21}}\left(\frac{h_f^3}{12}\right)+\frac{E_u}{1-\nu_u^2}\left(\frac{h_u^3}{3}+\frac{h_u^2h_f}{2}+\frac{h_uh_f^2}{4}\right)\end{array}\right)\frac{\partial^4 w}{\partial x^4}\\ +\left(\begin{array}{l}\frac{E_1}{1-\nu_1^2}\left(\frac{h_1^3}{3}+\frac{h_1^2h_f}{2}+\frac{h_1h_f^2}{4}\right)+\frac{E_{f2}}{1-\nu_{f12}\nu_{f21}}\left(\frac{h_f^3}{12}\right)+\\ \frac{E_{c2}}{1-\nu_{c12}\nu_{c21}}\left(\frac{h_f^3}{12}\right)+\frac{E_u}{1-\nu_u^2}\left(\frac{h_u^3}{3}+\frac{h_u^2h_f}{2}+\frac{h_uh_f^2}{4}\right)\end{array}\right)\frac{\partial^4 w}{\partial x^4}\\ +\left(\begin{array}{l}\frac{2E_1}{(1+\nu_1)}\left(\frac{h_1^3}{3}+\frac{h_1^2h_f}{2}+\frac{h_1h_f^2}{4}\right)+G_f\left(\frac{h_f^3}{3}\right)+\\ G_c\left(\frac{h_f^3}{3}\right)+\frac{2E_u}{(1+\nu)}\left(\frac{h_u^3}{3}+\frac{h_u^2h_f}{2}+\frac{h_uh_f^2}{4}\right)\end{array}\right)\frac{\partial^4 w}{\partial x^2\partial y^2}\end{array}\right)+\left(\rho_1h_1+\rho_fh_f+\rho_ch_f+\rho_uh_u\right)\frac{\partial^2 w}{\partial t^2}=0 \tag{13}$$

The above outcome is a 4th order equation, with a solution of method of separation of variables assumption, as a function of displacement with variables x, y and function of time of t variable. With the applied condition for a supported plate, the displacement equation can be written as [48],

$$w = Sin\frac{m\pi x}{a}Sin\frac{n\pi y}{b} \tag{14}$$

Substitution the Eq. (14) in 4th order Eq. (13), get,

$$\left(\left(\begin{array}{l}\left(\begin{array}{l}\frac{E_1}{1-\nu_1^2}\left(\frac{h_1^3}{3}+\frac{h_1^2h_f}{2}+\frac{h_1h_f^2}{4}\right)+\frac{E_{f1}}{1-\nu_{f12}\nu_{f21}}\left(\frac{h_f^3}{12}\right)+\\ \frac{E_{c1}}{1-\nu_{c12}\nu_{c21}}\left(\frac{h_f^3}{12}\right)+\frac{E_u}{1-\nu_u^2}\left(\frac{h_u^3}{3}+\frac{h_u^2h_f}{2}+\frac{h_uh_f^2}{4}\right)\end{array}\right)\left(\frac{m^4\pi^4}{a^4}\right)\\ +\left(\begin{array}{l}\frac{E_1}{1-\nu_1^2}\left(\frac{h_1^3}{3}+\frac{h_1^2h_f}{2}+\frac{h_1h_f^2}{4}\right)+\frac{E_{f2}}{1-\nu_{f12}\nu_{f21}}\left(\frac{h_f^3}{12}\right)+\\ \frac{E_{c2}}{1-\nu_{c12}\nu_{c21}}\left(\frac{h_f^3}{12}\right)+\frac{E_u}{1-\nu_u^2}\left(\frac{h_u^3}{3}+\frac{h_u^2h_f}{2}+\frac{h_uh_f^2}{4}\right)\end{array}\right)\left(\frac{n^4\pi^4}{b^4}\right)\\ +\left(\begin{array}{l}\frac{2E_1}{(1+\nu_1)}\left(\frac{h_1^3}{3}+\frac{h_1^2h_f}{2}+\frac{h_1h_f^2}{4}\right)+G_f\left(\frac{h_f^3}{3}\right)+\\ G_c\left(\frac{h_f^3}{3}\right)+\frac{2E_u}{(1+\nu)}\left(\frac{h_u^3}{3}+\frac{h_u^2h_f}{2}+\frac{h_uh_f^2}{4}\right)\end{array}\right)\left(\frac{m^2n^2\pi^2}{a^2b^2}\right)\\ \left(\rho_1h_1+\rho_fh_f+\rho_ch_f+\rho_uh_u\right)\frac{\partial^2 w}{\partial t^2}\end{array}\right)w\right)=0 \tag{15}$$

By comparison, the resultant equation with the 2nd order simple form, the result ω_{mn}^2 can be easily recognized,

$$\omega_{mn}^2=\frac{\left(\begin{array}{l}\frac{E_1}{1-\nu_1^2}\left(\frac{h_1^3}{3}+\frac{h_1^2h_f}{2}+\frac{h_1h_f^2}{4}\right)+\frac{E_{f1}}{1-\nu_{f12}\nu_{f21}}\left(\frac{h_f^3}{12}\right)+\frac{E_{c1}}{1-\nu_{c12}\nu_{c21}}\left(\frac{h_f^3}{12}\right)+\frac{E_u}{1-\nu_u^2}\left(\frac{h_u^3}{3}+\frac{h_u^2h_f}{2}+\frac{h_uh_f^2}{4}\right)\left(\frac{m\pi}{a}\right)^4\\ \frac{E_1}{1-\nu_1^2}\left(\frac{h_1^3}{3}+\frac{h_1^2h_f}{2}+\frac{h_1h_f^2}{4}\right)+\frac{E_{f2}}{1-\nu_{f12}\nu_{f21}}\left(\frac{h_f^3}{12}\right)+\frac{E_{c2}}{1-\nu_{c12}\nu_{c21}}\left(\frac{h_f^3}{12}\right)+\frac{E_u}{1-\nu_u^2}\left(\frac{h_u^3}{3}+\frac{h_u^2h_f}{2}+\frac{h_uh_f^2}{4}\right)\left(\frac{n\pi}{b}\right)^4\\ +\left(\frac{2E_1}{(1+\nu_1)}\left(\frac{h_1^3}{3}+\frac{h_1^2h_f}{2}+\frac{h_1h_f^2}{4}\right)+G_f\left(\frac{h_f^3}{3}\right)+G_c\left(\frac{h_f^3}{3}\right)+\frac{2E_u}{(1+\nu)}\left(\frac{h_u^3}{3}+\frac{h_u^2h_f}{2}+\frac{h_uh_f^2}{4}\right)\right)\left(\frac{mn\pi^2}{ab}\right)^2\end{array}\right)}{\left(\rho_1h_1+\rho_fh_f+\rho_ch_f+\rho_uh_u\right)} \tag{16}$$

A rectangular sandwich plate has a natural frequency of ω_{mn}. All edges have simply supported boundary conditions. Since $a = b$ rectangular plate, the upper face and lower are the same $h_l = h_u = h_s$, $\nu_{f12} = \nu_{f21} = \nu_f$, $E_{f1} = E_{f2} = E_f$, $\nu_{c12} = \nu_{c21} = \nu_c$ and $E_{c1} = E_{c2} = E_c$. Taking $m = 1$ and $n = 1$, the equation can be expressed as,

$$\omega_{mn}^2=\frac{\left(\frac{\pi}{a}\right)^4\left(2\left(\frac{2E_s}{1-\nu_s^2}\right)\left(\frac{h_s^3}{3}+\frac{h_s^2h_f}{2}+\frac{h_sh_f^2}{4}\right)+\left(\frac{h_f^3}{12}\right)\left(\frac{E_f}{1-\nu_c^2}+\frac{E_c}{1-\nu_c^2}\right)+\left(\frac{4E_1}{(1+\nu_s)}\right)\left(\frac{h_s^3}{3}+\frac{h_s^2h_f}{2}+\frac{h_sh_f^2}{4}\right)+\left(\frac{h_f^3}{3}\right)(G_f+G_c)\right)}{2\rho_sh_s+h_f(\rho_f+\rho_c)} \tag{17}$$

To calculate the mechanical performance of the hybrid core, for the open structure part relying on the equation of the open structure, open-cell design,

$$E_{c2}^*=E_{c1}^*=E_c^*=\left(\frac{1}{c^2h}\left(\begin{array}{l}t\left(c^2-\left(c-\frac{t}{2}\right)+\left(c^2-(c-t)\right)\right)\\ +t^2\left(\sqrt{2c^2+(h-2t)^2}-\frac{t}{\tan\gamma}\right)\end{array}\right)\right)^2E_c \tag{18}$$

$$\frac{\rho^*}{\rho_0}=\frac{1}{c^2h}\left(\begin{array}{l}t\left(\left(c^2-\left(c-\frac{t}{2}\right)\right)+\left(c^2-(c-t)\right)\right)\\ +t^2\left(\sqrt{2c^2+(h-2t)^2}-\frac{t}{\tan\gamma}\right)\end{array}\right)^2E_c \tag{19}$$

To make Eq. 16, which has already been derived, more suitable for the hybrid core layer situation, the variables of that layer are exchanged according to Eqs. 18 and 19,

$$\omega_{11}^{2}=\frac{\left(\frac{\pi}{a}\right)^{4}\left(2\left(\frac{2E_{s}}{1-\nu_{s}^{2}}\right)\left(\frac{h_{s}^{3}}{3}+\frac{h_{s}^{2}h_{f}}{2}+\frac{h_{s}h_{f}^{2}}{4}\right)+\left(\frac{h_{f}^{3}}{12}\right)\left(\frac{E_{f}^{*}}{1-\nu_{c}^{2}}+\frac{E_{c}^{*}}{1-\nu_{c}^{2}}\right)+\left(\frac{4E_{1}}{(1+\nu_{s})}\right)\left(\frac{h_{s}^{3}}{3}+\frac{h_{s}^{2}h_{f}}{2}+\frac{h_{s}h_{f}^{2}}{4}\right)\right)}{2\rho_{s}h_{s}+h_{f}\left(\rho_{f}+\rho_{c}\right)} \tag{20}$$

4. Numerical Investigation

As car companies work on a new idea, a concept is built (prototype) to visualize dimensions and asymmetrical lines to describe an idea and bring it closer to reality. To merge theoretical analysis into reality by making a digital replica to be analyzed [49]. Once the constituent materials are simulated and their mechanical properties are specified and then analyzed using a simulation (program), results that support the analytical results appear more realistically. The finite element method (FEM) is a numerical solving approach for complex engineering problems and experiments, and ANSYS 2021-R1 software was employed for this work. The model must be designed to analyze with ANSYS software, and then properties and boundary conditions must be specified [50]. Once it is completed then simulation was performed to obtain results. Fig. 4 demonstrates models created for the sandwich plate.

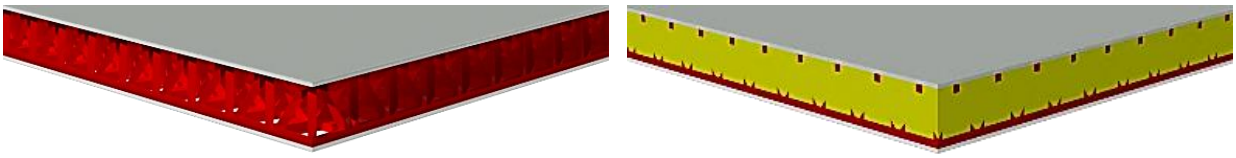

a. Open-Cell **b. Open-cell with foam materials**

Fig. 4. Models of sandwich used

From the ANSYS software library, which contains many elements that are distinguished from each other by criteria such as geometry, i.e., two-dimensional or three-dimensional, as well as the degree of freedom (DOF), one of these elements is selected through which the analysis is carried out. The primary element that was adopted for this analysis is SOLID186. The aspect is characterized by having 3DOF to transfer in the direction (x, y, and z) for each node, and it contains twenty nodes. Fig. 5 demonstrates the element SOLID186. Matter changes by changing its properties. Materials can have orthotropic or isotropic properties; some properties vary while others remain constant [51]. Materials' properties are to be archived in ANSYS or already in the program Library. The chosen material's characteristics are listed in Table 1.

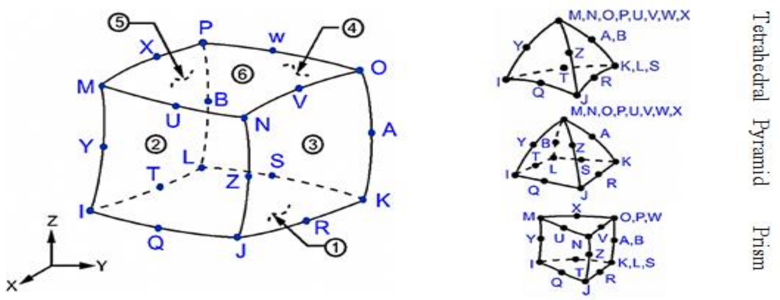

Fig. 5. ANSYS Element SOLID186.

Table 1. The sandwich plate model chosen materials' characteristics

Layer	E (GPa)	ρ Kg/m³	ν_s	h (mm)
Al	61.25	2710	0.33	1
Foam (PU)	0.0382	100	0.3	14
Open cell-PLA	1.172	1360	0.3	14
Open cell-TPU	0.833	1450	0.3	14

Meshing is to break the model into small parts grouped within a network. Increasing the mesh elements means more accuracy in the solution, but it requires a longer time to model it. Unlike the old versions, the ANSYS 2021-R1 workbench figures out mesh element size in an auto manner with the default element type SOLID186. Simply supported as boundary conditions were employed in all FEA cases. The sandwich plate has elements up to 12500 and 59211 nodes. The FEM model mesh is demonstrated in Fig. 6. The study of free vibration for any structure includes calculating the mode shape, thus calculating the natural frequency for all modes. These modes can easily illustrate the deflection the plate exhibits. The numerical analysis steps in ANSYS software include the geometry of the model, FEM mesh generating, locating the boundary conditions, and deformation mode shapes as an output.

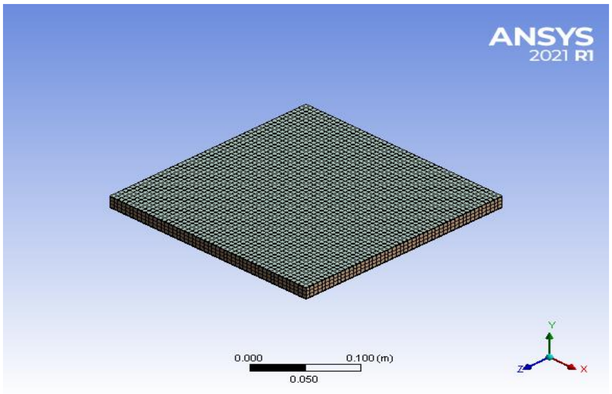

Fig. 6. The FEM model mesh

5. Results

Table 2 states the result of natural frequency for hybrid structure. Both the structure and the foam have unique qualities that set them apart. By combining the two into a hybrid system, these qualities may be used to create a high-quality design. The change in the elastic modulus depends on the change in the density of both foam and cellular structure. Increasing the foam density from 60, 100, 150, ..., 400, and 450 kg/m^3 leads to an improvement in the elastic modulus and thus reduces the natural frequency by 1.4%, 3.2%, 4.8%, 6.4%, 7.8%, 9.2%, 10.6% and 11.8%, respectively. Figure 10 demonstrates the relation between the hybrid structure's elastic modulus and natural frequency. Figure 11 demonstrates the relation between the change in foam density and the natural frequency of the hybrid structure.

When observing the results obtained through the numerical analysis, their behavior tends to match the behavior of the results of the analytical analysis but deviates with a slight discrepancy. The discrepancy can be traced back to the material's characteristics, hypotheses in the analytical analysis, and core structure. The discrepancy in the analytical and numerical results was below 6%. The numerical solution results and discrepancies are inserted in Table 3.

Table 2. Results of the natural frequencies for the hybrid structure

Material	PUR E_f (GPa)	PUR ρ_f (kg/m^3)	Hybrid E_f* PUR GPa	Hybrid PUR ν_f*	Hybrid PUR ρ_f* (kg/m^3)	G_f* (GPa)	Analytical ω_n (rad/sec)
PLA	0.0045	60	0.003	0.3	40.262	0.002	7278.69
	0.0382	100	0.026		67.104	0.018	7173.14
	0.0595	150	0.040		100.656	0.029	7045.52
	0.0922	200	0.062		134.208	0.044	6925.81
	0.1276	250	0.086		167.760	0.061	6812.49
	0.173	300	0.116		201.312	0.083	6705.77
	0.2229	350	0.150		234.864	0.107	6604.63
	0.269	400	0.181		268.416	0.129	6507.84
	0.3229	450	0.217		301.968	0.155	6416.17
TPU	0.0045	60	0.003		40.262	0.002	7154.21
	0.0382	100	0.026		67.104	0.018	7053.90
	0.0595	150	0.040		100.656	0.029	6932.36
	0.0922	200	0.062		134.208	0.044	6818.20

0.1276	250	0.086	167.760	0.061	6709.97
0.173	300	0.116	201.312	0.083	6607.94
0.2229	350	0.150	234.864	0.107	6511.12
0.269	400	0.181	268.416	0.129	6418.33
0.3229	450	0.217	301.968	0.155	6330.38

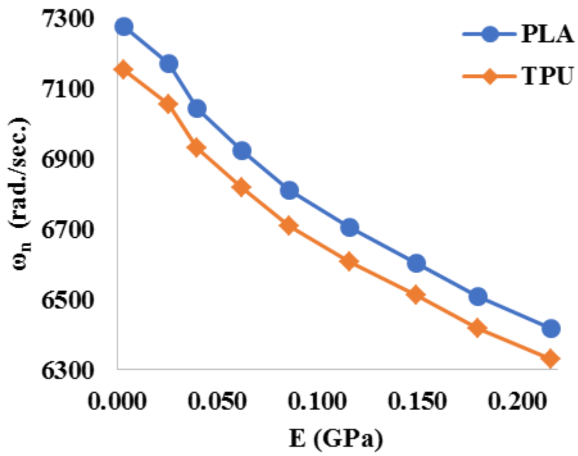

Fig. 10. Elastic modulus vs. natural frequency of the hybrid structure

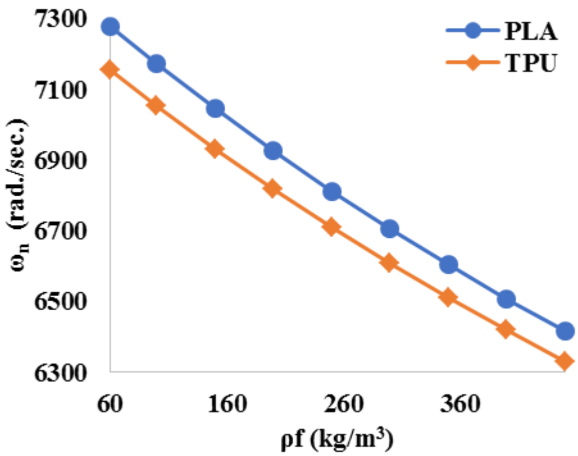

Fig. 11. Density vs. natural frequency relation of the hybrid structure

Table 3: Frequency results of the numerical solution

Type	Analytical ω_n (rad/sec)	Numerical ω_n (rad/sec)	Discrepancy (%)
Hybrid PUR-TPU	7053.89	7439.04	5.46
Hybrid PUR-PLA	7173.13	7564.79	5.46

6. Conclusions

An analytical model is utilized to conduct an analysis of the free vibration of composite SPs that has been subjected to simply supported boundary conditions according to the generalized Hooke's rule, within the framework of CPT. Mechanical properties, and natural frequency were estimated. Consideration is given to three types of core arrangement. The accuracy of the new approach is simulated by using FEM and the results of natural frequency are compared based on various types of hybrid cores these conditions feature distinct mechanical behaviour of composite sandwich plates. It has been determined that this method produces satisfactory outcomes. The most important conclusions obtained from this study are recoded below:

1. Converting a solid material or replacing a foam form with a cellular pattern is very effective by reducing both mass cost and maintaining its performance.
2. Hybrid structures provide a great combination to improve mechanical characteristics.
3. The natural frequency of the hybrid structure is reduced by 27.6%.
4. The ultimate flexural load in the hybrid structure is increased by 127.7% compared to the open-cell structure core, and the maximum deflection is also increased by 163.3%.

Acknowledgements

The authors are grateful to the University of Kufa, College of Engineering/ Iraq, for providing facilities to carry out this work.

References

[1] M. Jafari, A. Kaveh, A. Ardebili, O. Moini Jazani, Design and simulation Sandwich Composite Fairing Shells Using FEM Analyzing, *Journal of Computational Applied Mechanics,* Vol. 53, No. 1, pp. 55-65, 2022.

[2] A. M. Zenkour, H. D. El-Shahrany, Forced vibration of a magnetoelastic laminated composite beam on Pasternak's foundation, *Journal of Computational Applied Mechanics,* Vol. 52, No. 3, pp. 478-497, 2021.

[3] M. Al-Shablle, E. K. Njim, M. J. Jweeg, M. Al-Waily, Free vibration analysis of composite face sandwich plate strengthens by Al2O3 and SiO2 nanoparticles materials, *Diagnostyka,* Vol. 24, No. 2, pp. 1-9, 2023.

[4] J. Zhao, Z. Cui, S. Wang, Z. Sun, Y. Ding, Flexural response of additively manufactured honeycomb sandwich structures with continuous density-gradient variations, *Thin-Walled Structures,* Vol. 197, pp. 111642, 2024/04/01/, 2024.

[5] Y. Li, W. Xiao, X. Wu, L. Zhu, Analytical study on the dynamic response of foam-core sandwich plate under wedge impact, *International Journal of Impact Engineering,* Vol. 173, pp. 104464, 2023/03/01/, 2023.

[6] B. Sture, L. Vevere, M. Kirpluks, D. Godina, A. Fridrihsone, U. Cabulis, Polyurethane Foam Composites Reinforced with Renewable Fillers for Cryogenic Insulation, *Polymers,* Vol. 13, No. 23, pp. 4089, 2021.

[7] X. Zheng, Z. Xiao, Z. Ren, B. Zi, H. Bai, Y. Wu, L. Yao, Low-velocity impact response of sandwich structures with cores made from entangled metallic wire material - silicone rubber composites, *Construction and Building Materials,* Vol. 431, pp. 136633, 2024/06/14/, 2024.

[8] Z. Zheng, H.-S. Shen, H. Wang, X. Chen, T. Lu, Nonlinear low-velocity impact analysis of sandwich plates with titanium face sheets and porous aluminum core reinforced by GPLs, *Alexandria Engineering Journal,* Vol. 93, pp. 207-219, 2024/04/01/, 2024.

[9] S. Yang, H. Luo, L. Wang, J. Wu, Y. Mu, L. Wu, Interface microstructures and mechanical properties of foamable precursor sandwiches and aluminum foam sandwiches, *Composite Structures,* Vol. 336, pp. 117961, 2024/05/15/, 2024.

[10] D. Duryodhana, S. Waddar, D. Bonthu, J. Pitchaimani, S. Powar, M. Doddamani, Buckling and free vibrations behaviour through differential quadrature method for foamed composites, *Results in Engineering,* Vol. 17, pp. 100894, 2023/03/01/, 2023.

[11] K. Guo, L. Zhu, Y. Li, T. X. Yu, A. Shenoi, Q. Zhou, Experimental investigation on the dynamic behaviour of aluminum foam sandwich plate under repeated impacts, *Composite Structures,* Vol. 200, pp. 298-305, 2018/09/15/, 2018.

[12] C. Caglayan, I. Osken, A. Ataalp, H. S. Turkmen, H. Cebeci, Impact response of shear thickening fluid filled polyurethane foam core sandwich composites, *Composite Structures,* Vol. 243, pp. 112171, 2020/07/01/, 2020.

[13] P. Ren, L. Yin, Q. Tao, Z. Guo, W. Zhang, Dynamic failure of carbon fiber-reinforced plastics sandwich structures with polyvinyl chloride foam cores subjected to impact loading, *Journal of Sandwich Structures & Materials,* Vol. 23, No. 6, pp. 2375-2398, 2021.

[14] A. Koyama, D. Suetsugu, Y. Fukubayashi, H. Mitabe, Experimental study on the dynamic properties of rigid polyurethane foam in stress-controlled cyclic uniaxial tests, *Construction and Building Materials,* Vol. 321, pp. 126377, 2022/02/28/, 2022.

[15] H. Raissi, M. Shishesaz, S. Moradi, Applications of higher order shear deformation theories on stress distribution in a five layer sandwich plate, *Journal of Computational Applied Mechanics,* Vol. 48, No. 2, pp. 233-252, 2017.

[16] F. Masmoudi, A. Tamrabet, S. Refrafi, N. Alselami, A. Menasria, A. Bouhadra, S. Benyoucef, Coupled loading hygro-thermo-mechanical Effect on the stability of imperfect functionally graded sandwich plates, *Journal of Computational Applied Mechanics,* pp. -, 2024.

[17] A. Tamrabet, C. Mourad, N. Ali Alselami, A. Menasria, B. Mamen, A. Bouhadra, Efficient Kinematic model for Stability Analysis of Imperfect Functionally Graded Sandwich Plates with Ceramic middle layer and Varied Boundary Edges, *Journal of Computational Applied Mechanics,* Vol. 55, No. 2, pp. 184-200, 2024.

[18] A. Ghaznavi, M. Shariyat, Real Time Finite Element Simulation of Thick and Thin Sandwich Plate with Viscoelastic Core and Embedded SMA Wires, *Journal of Computational Applied Mechanics,* Vol. 53, No. 2, pp. 219-243, 2022.

[19] E. K. Njim, S. H. Bakhy, M. Al-Waily, Analytical and Numerical Investigation of Free Vibration Behavior for Sandwich Plate with Functionally Graded Porous Metal Core, *Pertanika Journal of Science and Technology,* 2021.

[20] S. Maraş, M. Yaman, Experimental and numerical investigation of free vibration behaviours of sandwich syntactic foams, *Structures,* Vol. 58, pp. 105390, 2023/12/01/, 2023.

[21] N.-D. Nguyen, V.-T. Bui, T.-K. Nguyen, A modified strain gradient theory for buckling, bending and free vibration behaviors of metal foam microbeams, *Structures,* Vol. 64, pp. 106533, 2024/06/01/, 2024.

[22] J. Sun, L. Yan, K. Zhu, P. Jiang, Y. Xu, X. Zheng, An all-composite sandwich structure with PMI foam-filled for adjustable vibration suppression and improved mechanical properties, *Thin-Walled Structures,* Vol. 196, pp. 111544, 2024/03/01/, 2024.

[23] Z. Li, H. Li, Y. Yang, Y. Deng, Z. Zhang, C. Ren, H. Wang, B. Zhou, J. Zhou, H. Wang, H. Zhang, Z. Luo, Q. Han, Z. Guan, Nonlinear vibration behaviours of foam-filled honeycomb sandwich cylindrical shells: Theoretical and experimental investigations, *Aerospace Science and Technology*, pp. 109252, 2024/05/28/, 2024.

[24] M. Arabzadeh-Ziari, M. Mohammadimehr, E. Arabzadeh-Ziari, M. Asgari, Deflection, buckling and vibration analyses for a sandwich nanocomposite structure with foam core reinforced with GPLs and SMAs based on TSDBT, *Journal of Computational Applied Mechanics,* Vol. 55, No. 2, pp. 289-321, 2024.

[25] A. Farazin, A. H. Ghasemi, N. Miralaei, A. Yvaz, Investigation of the effect of impactor shape on the behavior of composite sandwich plates with aluminum foam core at low-speed impact: Experimental and physical study, *Journal of Computational Applied Mechanics,* Vol. 54, No. 1, pp. 150-166, 2023.

[26] M. S. H. Al-Furjan, C. Yin, X. Shen, R. Kolahchi, M. S. Zarei, M. H. Hajmohammad, Energy absorption and vibration of smart auxetic FG porous curved conical panels resting on the frictional viscoelastic torsional substrate, *Mechanical Systems and Signal Processing,* Vol. 178, pp. 109269, 2022/10/01/, 2022.

[27] M. S. H. Al-Furjan, Y. Yang, A. Farrokhian, X. Shen, R. Kolahchi, D. K. Rajak, Dynamic instability of nanocomposite piezoelectric-leptadenia pyrotechnica rheological elastomer-porous functionally graded materials micro viscoelastic beams at various strain gradient higher-order theories, *Polymer Composites*, Vol. 43, No. 1, pp. 282-298, 2022.

[28] M. S. H. Al-Furjan, L. Shan, X. Shen, R. Kolahchi, D. K. Rajak, Combination of FEM-DQM for nonlinear mechanics of porous GPL-reinforced sandwich nanoplates based on various theories, *Thin-Walled Structures*, Vol. 178, pp. 109495, 2022/09/01/, 2022.

[29] M. Mohammadi, A. Farajpour, A. Moradi, M. Ghayour, Shear buckling of orthotropic rectangular graphene sheet embedded in an elastic medium in thermal environment, *Composites Part B: Engineering,* Vol. 56, pp. 629-637, 2014/01/01/, 2014.

[30] M. Mohammadi, A. Farajpour, A. Rastgoo, Coriolis effects on the thermo-mechanical vibration analysis of the rotating multilayer piezoelectric nanobeam, *Acta Mechanica,* Vol. 234, No. 2, pp. 751-774, 2023/02/01, 2023.

[31] M. Mohammadi, A. Farajpour, A. Moradi, M. Hosseini, Vibration analysis of the rotating multilayer piezoelectric Timoshenko nanobeam, *Engineering Analysis with Boundary Elements,* Vol. 145, pp. 117-131, 2022/12/01/, 2022.

[32] M. Mohammadi, M. Goodarzi, M. Ghayour, A. Farajpour, Influence of in-plane pre-load on the vibration frequency of circular graphene sheet via nonlocal continuum theory, *Composites Part B: Engineering,* Vol. 51, pp. 121-129, 2013/08/01/, 2013.

[33] M. Mohammadi, M. Hosseini, M. Shishesaz, A. Hadi, A. Rastgoo, Primary and secondary resonance analysis of porous functionally graded nanobeam resting on a nonlinear foundation subjected to mechanical and electrical loads, *European Journal of Mechanics - A/Solids,* Vol. 77, pp. 103793, 2019/09/01/, 2019.

[34] H. Moosavi, M. Mohammadi, A. Farajpour, S. H. Shahidi, Vibration analysis of nanorings using nonlocal continuum mechanics and shear deformable ring theory, *Physica E: Low-dimensional Systems and Nanostructures,* Vol. 44, No. 1, pp. 135-140, 2011/10/01/, 2011.

[35] M. Mohammadi, M. Safarabadi, A. Rastgoo, A. Farajpour, Hygro-mechanical vibration analysis of a rotating viscoelastic nanobeam embedded in a visco-Pasternak elastic medium and in a nonlinear thermal environment, *Acta Mechanica*, Vol. 227, No. 8, pp. 2207-2232, 2016/08/01, 2016.

[36] M. S. H. Al-Furjan, R. Kolahchi, L. Shan, M. H. Hajmohammad, A. Farrokhian, X. Shen, Slamming impact induced hydrodynamic response in wave-piercing catamaran beam elements with controller, *Ocean Engineering,* Vol. 266, pp. 112908, 2022/12/15/, 2022.

[37] M. Motezaker, R. Kolahchi, D. K. Rajak, S. R. Mahmoud, Influences of fiber reinforced polymer layer on the dynamic deflection of concrete pipes containing nanoparticle subjected to earthquake load, *Polymer Composites,* Vol. 42, No. 8, pp. 4073-4081, 2021.

[38] M. S. H. Al-Furjan, Z. H. Qi, L. Shan, A. Farrokhian, X. Shen, R. Kolahchi, Nano supercapacitors with practical application in aerospace technology: Vibration and wave propagation analysis, *Aerospace Science and Technology,* Vol. 133, pp. 108082, 2023/02/01/, 2023.

[39] R. Kolahchi, B. Keshtegar, N.-T. Trung, Optimization of dynamic properties for laminated multiphase nanocomposite sandwich conical shell in thermal and magnetic conditions, *Journal of Sandwich Structures & Materials,* Vol. 24, No. 1, pp. 643-662, 2022.

[40] L. Shan, C. Y. Tan, X. Shen, S. Ramesh, M. S. Zarei, R. Kolahchi, M. H. Hajmohammad, The effects of nano-additives on the mechanical, impact, vibration, and buckling/post-buckling properties of composites: A review, *Journal of Materials Research and Technology,* Vol. 24, pp. 7570-7598, 2023/05/01/, 2023.

[41] C. Chu, L. Shan, M. S. H. Al-Furjan, M. S. Zarei, M. H. Hajmohammad, R. Kolahchi, Experimental study for the effect of hole notched in fracture mechanics of GLARE and GFRP composites subjected to quasi-static loading, *Theoretical and Applied Fracture Mechanics,* Vol. 122, pp. 103624, 2022/12/01/, 2022.

[42] L. Hadji, R. Madan, F. Bernard, Thermal buckling in multi-directional porous plates: The effects of material grading and aspect ratio, *Proceedings of the Institution of Mechanical Engineers, Part G: Journal of Aerospace Engineering,* Vol. 238, No. 4, pp. 412-426, 2024.

[43] L. Hadji, V. Plevris, R. Madan, H. Ait Atmane, Multi-Directional Functionally Graded Sandwich Plates: Buckling and Free Vibration Analysis with Refined Plate Models under Various Boundary Conditions, *Computation,* Vol. 12, No. 4, pp. 65, 2024.

[44] R. Madan, S. Bhowmick, L. Hadji, A. Alnujaie, Limit angular speed analysis of porous functionally graded rotating disk under thermo-mechanical loading, *Multidiscipline Modeling in Materials and Structures,* Vol. 19, No. 2, pp. 311-323, 2023.

[45] E. Kadum Njim, M. J. Jweeg, M. H. Al-Maamori, Z. S. Idan, M. Al-Waily, A. Mouthanna, L. Hadji, Wear Behavior Analysis of Imperfect Functionally Graded Parts: Analytical and Experimental Techniques, *BIO Web Conf.,* Vol. 97, pp. 00001, 2024.

[46] M. S. H. Al-Furjan, M. X. Xu, A. Farrokhian, G. S. Jafari, X. Shen, R. Kolahchi, On wave propagation in piezoelectric-auxetic honeycomb-2D-FGM micro-sandwich beams based on modified couple stress and refined zigzag theories, *Waves in Random and Complex Media,* pp. 1-25.

[47] E. K. Njim, S. H. Bakhy, M. Al-Waily, Analytical and Numerical Investigation of Buckling Behavior of Functionally Graded Sandwich Plate with Porous Core, *Journal of Applied Science and Engineering,* Vol. 25, No. 2, pp. 339-347, 2021/08/29, 2021.

[48] M. Al-Waily, H. Raad, E. K. Njim, Free Vibration Analysis of Sandwich Plate-Reinforced Foam Core Adopting Micro Aluminum Powder, *Physics and Chemistry of Solid State,* Vol. 23, No. 4, pp. 659-668, 11/30, 2022.

[49] S. Carusotti, R. Lombroni, P. Fanelli, L. Jackson, F. Giorgetti, P. F. Buxton, G. Calabrò, M. Romanelli, E. R. d. V. Valdes, Structural behaviour characterization of ST40 Inner Vacuum Chamber (IVC2) during a plasma VDE using ANSYS Workbench, *Fusion Engineering and Design,* Vol. 192, pp. 113772, 2023/07/01/, 2023.

[50] A. Mouthanna, S. H. Bakhy, M. Al-Waily, E. K. Njim, Free Vibration Investigation of Single-Phase Porous FG Sandwich Cylindrical Shells: Analytical, Numerical and Experimental Study, *Iranian Journal of Science and Technology, Transactions of Mechanical Engineering,* 2023/08/29, 2023.

[51] E. K. Njim, H. R. Hasan, M. J. Jweeg, M. Al-Waily, A. A. Hameed, A. M. Youssef, F. M. Elsayed, Mechanical Properties of Sandwiched Construction with Composite and Hybrid Core Structure, *Advances in Polymer Technology,* Vol. 2024, No. 1, pp. 3803199, 2024.